Original Article

Institution of MECHANICAL ENGINEERS
Journal of SYSTEMS AND CONTROL ENGINEERING

Proc IMechE Part I:
J Systems and Control Engineering
2019, Vol. 233(10) 1298–1308

DOI: 10.1177/0959651819828460
journals.sagepub.com/home/pii
SAGE

A distributed swarm control for an agricultural multiple unmanned aerial vehicle system

Chanyoung Ju and Hyoung Il Son

Abstract

In this study, we propose a distributed swarm control algorithm for an agricultural multiple unmanned aerial vehicle system that enables a single operator to remotely control a multi-unmanned aerial vehicle system. The system has two control layers that consist of a teleoperation layer through which the operator inputs teleoperation commands via a haptic device and an unmanned aerial vehicle control layer through which the motion of unmanned aerial vehicles is controlled by a distributed swarm control algorithm. In the teleoperation layer, the operator controls the desired velocity of the unmanned aerial vehicle by manipulating the haptic device and simultaneously receives the haptic feedback. In the unmanned aerial vehicle control layer, the distributed swarm control consists of the following three control inputs: (1) velocity control of the unmanned aerial vehicle by a teleoperation command, (2) formation control to obtain the desired formation, and (3) collision avoidance control to avoid obstacles. The three controls are input to each unmanned aerial vehicle for the distributed system. The proposed algorithm is implemented in the dynamic simulator using robot operating system and Gazebo, and experimental results using four quadrotor-type unmanned aerial vehicles are presented to evaluate and verify the algorithm.

Keywords

Agricultural unmanned aerial vehicle, multi-unmanned aerial vehicle system, distributed swarm control, haptic teleoperation, unmanned aerial vehicle simulator

Date received: 22 May 2018; accepted: 10 January 2019

Introduction

Automated smart farm attracts increasing attention because it replaces the decreasing agricultural population by utilizing various sensors, big data, drones, and unmanned robots and can improve the efficiency of agricultural work to prepare for food shortages in the future. Given this, various studies focus on robotization and automation technology of agriculture with respect to existing agricultural methods using agricultural robots. Future developments in the agricultural environments are expected to center on these advanced systems.[1,2]

When drones or unmanned aerial vehicles (UAVs) are used in agricultural fields, it is possible to create a map that reconstructs the location of farmland and crops in three dimensions (3D). Subsequently, the yield of crops is estimated through sensors mounted on the UAV.[3] Furthermore, the health index and vegetation index of crops are calculated through visual, infrared, and thermal information measured by the UAV. Agricultural production and distribution strategies are established by the UAV in real time.[4] In addition, the method using agricultural UAV more accurately detects pests and diseases that cannot be observed well on the ground and facilitate eco-friendly and high-efficiency agriculture by applying variable amounts of water, fertilizer, and pesticide based on the state of the crop.[5] It also applies to other tasks, such as soil and farmland investigation or monitoring and sowing. Thus, agricultural UAVs display excellent potential in addition to low maintenance costs that are used in a variety of farming applications and are growing rapidly as a major technology for smart farming.[6]

Department of Rural and Biosystems Engineering, Chonnam National University, Gwangju, Republic of Korea

Corresponding author:
Hyoung Il Son, Department of Rural and Biosystems Engineering, Chonnam National University, Gwangju 61186, Republic of Korea.
Email: hison@jnu.ac.kr

However, an individual UAV involves limitations in terms of weight, size, and energy consumption for itself as well as for the sensors that it carries.[7] Furthermore, the battery limit of the UAV reduces agricultural efficiency when farming on a wide farmland due to the short time of flight. For example, a UAV for spraying can fly for approximately 10–15 min per battery and approximately corresponds to 8 min on an average per hectare. In this case, batteries must be exchanged unconditionally during agricultural tasks when a UAV is sprayed over 2 ha of farmland because the thrust of the UAV becomes weak and returns to the starting point when the battery is insufficient. These tasks delay the time of agricultural work and reduce efficiency. Furthermore, when a UAV is used for air transport, it is unable to transport crops or certain objects that are heavier than its payload.

A method to alleviate these problems involves performing farming using multiple robots that cooperate to achieve the mission goal (i.e. crop scouting, seeding, pesticide spraying, and transport). Various performance improvements occur when a multi-UAV system that can improve robustness is used and include a reduction in the completion time and an increase in the amount of workload relative to a time when compared to those when a single UAV system is applied.[8–11] Specifically, it is possible to achieve high economic efficiency by cooperating with multiple UAVs in a large area. Therefore, the deployment of multiple UAVs further increases agricultural working efficiency by utilizing the advantages of a multi-robot system. The applications of multi-UAV systems are used for detecting, localizing, tracking, surveillance, and intercepting.[12–14] However, in a few cases, the multi-UAV system was applied to agriculture and several studies continue to progress (e.g. multi-UAV-based cooperative remote sensing for real-time water management and irrigation control). Hence, various studies are currently underway to develop an agricultural multi-UAV system.[15] In this study, we propose a swarm control algorithm that is applied to a multi-UAV system for agriculture.

If a multi-UAV system is introduced in agricultural environments (e.g. multiple UAVs simultaneously spray water, scout crops, and detect pest), a more advanced and smarter system is constructed when compared with the current agricultural environment. However, several difficulties persist in the actual application of the agricultural multi-UAV system. Thus, to adapt to the real agricultural environment, we designed a multi-UAV system by considering the following two methods (1) a UAV control method and (2) a swarm control method. The first method (UAV control method) involves three typical methods to control the UAV, namely a method of fully autonomous driving using simultaneous localization and mapping (SLAM), a method of driving on a certain path as specified by the operator based on Global Positioning System (GPS), and a method of teleoperation by the operator in real time. Currently, most methods of controlling UAV in agriculture use the second method using ground station software such as *Mission Planner* or *QGroundControl*. However, this method specifies the path each time, and thus, the system becomes more complicated and difficult when the use of the UAVs increases, and it usually uses a centralized controller while attempting to control multi-UAV. Therefore, it is not suitable to use agricultural multiple UAVs. The best method involves performing agricultural tasks with fully automated UAVs. Unfortunately, it is not currently possible to guarantee the safety of using multiple UAVs that automatically avoid obstacles and fly the path using SLAM or machine vision (MV) in unstructured, unspecified, and uncertain agricultural environments. Furthermore, it is difficult to cope with unpredictable errors or accidents (e.g. collisions between UAVs). In such cases, fully autonomous control of the UAVs is typically infeasible/impossible, and instead, a teleoperation of their behaviors is desired if not absolutely necessary to impose human intelligence on the task of coping with the aforementioned uncertainties.[16–19] Therefore, in this study, we only considered the method of teleoperation by the operator.

In case of teleoperation method, efficiency decreases and costs increase when several operators are mobilized to control multiple UAVs. Thus, an efficient system in which multiple UAVs are remotely controlled by a single operator is required.[20] In Chao et al.[15] and Avellar et al.,[21] several operators were mobilized to control an agricultural multi-UAV used for area coverage and remote sensing. Furthermore, the method that is most commonly used in agriculture currently is the 1:1 control method. Nevertheless, the proposed method in this study corresponds to a 1:N swarm control method in which it is not necessary to mobilize several operators. In the study, we considered a swarm control method involving the agricultural environment. The following three typical methods exist for swarm control: centralized method, decentralized method, and distributed method. The centralized method is a way to handle and control the whole process by a single reader that contains complete information. This method is relatively easy in terms of implementation of the system and management of data. However, the centralized method is not suitable for outdoor environments, such as agriculture, owing to the lack of a direct connection between UAVs. Thus, swarm control is not performed when an error occurs in the leader as well as when an error occurs in only a single UAV.[22] The distributed method is a way to maintain the swarm control system even if a certain leader includes errors because the distributed controller is mounted in each UAV, and this method is the most stable way to cope with unpredictable errors or accidents in agriculture. The decentralized method is an intermediate method between the centralized method and the distributed method. Among the three methods, we swarm control agricultural multiple UAVs using a more stable and flexible distributed method, and this

system copes with the uncertainty in the agricultural environment.

In brief, the control method that is currently used is a 1:1 control for agricultural multiple UAVs via several operators, and a system that uses swarm control via a single operator does not exist yet. Therefore, in this study, we proposed a distributed swarm control for an agricultural multi-UAV system that enables a single operator to remotely control the multi-UAV. The distributed swarm control consists of the following three control inputs: (1) a velocity control of UAV using a teleoperation command, (2) a formation control to form the desired formation using a potential field, and (3) a collision avoidance control to avoid obstacles. In a teleoperation, an operator uses a haptic device to control a multi-UAV, and appropriate haptic feedback is given to an operator. Formation control forms a desired formation using a potential function that is defined as the relative distance between UAVs. Collision avoidance control automatically avoids obstacles via a repulsive potential field defined as the distance between UAVs and obstacles. The three control inputs are transferred to each UAV on the distributed system. The proposed control algorithm uses an effective UAV control method and swarm control method by considering the application to the agricultural environment and is applied regardless of the number of UAVs. In this article, we implemented a multi-UAV system with the proposed distributed swarm control algorithm into a dynamic simulator and subsequently performed experiments to verify and evaluate the algorithm.

The structure of this article is as follows. Section "Distributed swarm teleoperation" introduces the control architecture based on a distributed swarm control algorithm. Section "Evaluation of distributed swarm control" shows an overall hardware-in-the-loop simulation that includes an experiment setup, an experimental task, and data analysis. Finally, sections "Experimental results" and "Conclusion" show experimental results using four UAVs and discuss the conclusions of this study and future research directions, respectively.

Distributed swarm teleoperation

This section presents a teleoperation architecture with a distributed swarm control algorithm. A 3-degree-of-freedom (DOF) haptic device is used as a master and multiple UAVs are slaves. Hereafter, we briefly review the dynamics and control architecture and refer the reader to Lee et al.[19] for further details.

UAV dynamics and low-level control

We consider N quadrotor-type UAVs with 3-DOF Cartesian positions that are denoted by $p_i \in \Re^3$, $i = 1, 2, \ldots, N$. Flight control of UAVs is derived from the following under-actuated Lagrangian dynamics equation in $SE(3)$[23]

$$m_i \ddot{p}_i = -\lambda_i R_i e_3 + m_i g e_3 + \delta_i \quad (1)$$

$$J_i \dot{w}_i + S(w_i) J_i w_i = \gamma_i + \zeta_i \quad (2)$$

with the following attitude kinematic equation

$$\dot{R}_i = R_i S(w_i) \quad (3)$$

where $m_i > 0$ denotes mass, $p_i := [p_1; p_2; \ldots; p_N] \in \Re^{3N}$ denotes the Cartesian center-of-mass position represented in the north-east-down (NED) inertial frame $\{O\} := \{N^O, E^O, D^O\}$, $\lambda_i \in \Re$ denotes thrust control input, $R_i \in SO(3)$ denotes the rotational matrix describing the body frame $B := \{N^B, E^B, D^B\}$ of UAV w.r.t. to the inertial frame $\{O\}$, g is the gravitation constant, $e_3 = [0, 0, 1]^T$ denotes the basis vector representing the down direction and representing that thrust and gravity act in the D-direction, $J_i \in \Re^{3\times 3}$ denotes the UAV's inertia matrix w.r.t. the body frame $\{B\}$, $w_i \in \Re^3$ denotes the angular velocity of the UAV relative to the inertial frame $\{O\}$ represented in the body frame $\{B\}$, $\gamma_i \in \Re^3$ denotes the attitude torque control input, $\delta_i, \zeta_i \in \Re^3$ denote the aerodynamic perturbations, and $S(w_i) : \Re^3 \to so(3)$ denotes the skew-symmetric operator defined s.t. for $\alpha, \beta \in \Re^3$, $S(\alpha)\beta = \alpha \times \beta$. For typical UAV flying, $\delta_i, \zeta_i \approx 0$.

The relation between angular velocity, thrust, and torque of each propeller for low-level control input is as follows

$$\begin{pmatrix} \lambda_i \\ \tau_{i1} \\ \tau_{i2} \\ \tau_{i3} \end{pmatrix} = \begin{bmatrix} k & k & k & k \\ 0 & -L & 0 & L \\ L & 0 & -L & 0 \\ b & -b & b & -b \end{bmatrix} \begin{pmatrix} \omega_{i1}^2 \\ \omega_{i2}^2 \\ \omega_{i3}^2 \\ \omega_{i4}^2 \end{pmatrix} \quad (4)$$

where k and b are constants that determine the relationship between angular velocity, thrust and torque, L is the distance between the propeller and the center of the UAV, τ_{ij} denotes the torque in the roll, pitch, and yaw directions, and ω_{ij} denotes the angular velocity of each propeller. As a result, when the desired thrust and torque are determined, the desired low-level control input can be generated by controlling the motor through equation (4).

Distributed swarm control

Our goal involves using the distributed method as opposed to the centralized method to simultaneously control the 3-DOF Cartesian position of N UAVs. The distributed swarm control algorithm approaches the following three fundamental requirements: (1) UAV control, (2) formation control, and (3) obstacle avoidance control.[19,24]

First, to describe the method in which the UAVs are connected via communication to form the $N-$ nodes, we define the dynamic undirected *connectivity graph* $\mathcal{G} \triangleq \{\mathcal{V}, \mathcal{E}\}$ by the vertex set $\mathcal{V} \triangleq \{1, 2, \ldots, n\}$, representing the UAVs, and the edge set $\mathcal{E} \triangleq \{e_{ij} : i = 1, 2, \ldots, n, j \in \mathcal{N}_i\}$ representing the connectivity among

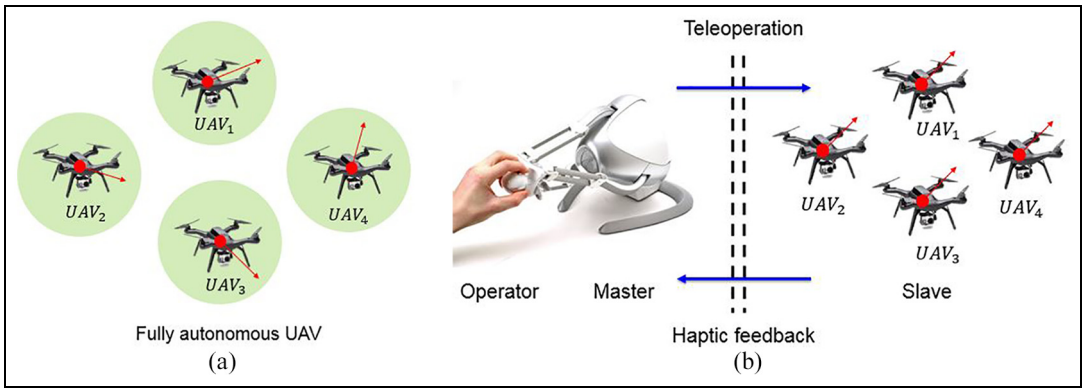

Figure 1. Concept of a multi-UAV system: (a) autonomous flight of multiple UAVs and (b) haptic teleoperation of multiple UAVs.

the UAVs, where the dynamic neighbor set $\mathcal{N}_i$ of UAV i is defined as follows

$$\mathcal{N}_i \triangleq \{j \in \mathcal{V} : i \text{ receivesinformationfrom } j,\ i \neq j\} \tag{5}$$

Subsequently, we implement the following distributed swarm control on each UAV, for the ith UAV

$$\dot{p}_i(t) := u_i^u + u_i^c + u_i^o \tag{6}$$

where the meaning of the three control inputs $u_i^u \in \Re^3$, $u_i^c \in \Re^3$, and $u_i^o \in \Re^3$ represents the velocity terms of the UAV.

UAV control, u_i^u. The UAV control method mainly uses the following three methods: (1) the method of fully autonomous driving, (2) the method of driving on a certain path specified by the operator, and (3) the method of teleoperation by the operator in real time (Figure 1). In case of (1), the position of the UAV $\hat{\mathbf{x}}_t$ at time t given the previous k positions $\mathbf{x}_{t-k:t-1}$ and the corresponding sensor measurements $b_{t-k:t}$, is as follows

$$\hat{\mathbf{x}}_t = \text{argmax}p(\mathbf{x}_t|\mathbf{x}_{t-k:t-1}, \mathbf{b}_{t-k:t}), \quad u_i^u = \dot{\mathbf{x}}_t \tag{7}$$

where $\mathbf{x}_t = (x_t, y_t, z_t)$. We briefly review the control of autonomous UAVs and refer the reader to Grzonka et al.[25] for further details. With respect to (2), the UAV typically follows the given path based on model predictive control (MPC) or nonlinear guidance law (NLGL) or potential field.[26] However, as mentioned in section "Introduction," we considered only the method of (3) given the agricultural environment.

Therefore, we consider a 3-DOF haptic device for master as modeled by the following nonlinear Lagrangian dynamics equation[27]

$$M(q)\ddot{q} + C(q, \dot{q})\dot{q} = \tau + f_h \tag{8}$$

where $q \in \Re^3$ denotes the configuration of the haptic device (e.g. the position of end effector), $M(q) \in \Re^{3\times3}$ denotes the positive-definite/symmetric inertia matrix, $C(q, \dot{q}) \in \Re^{3\times3}$ denotes the Coriolis matrix, and $\tau \in \Re^3$ and $f_h \in \Re^3$ denote the control input and human forces, respectively.

The velocity term, $u_i^u \in \Re^3$, represents the teleoperation command for the desired velocity input of the UAV that is directly controlled by the operator using the configuration of the haptic device q

$$u_i^u = \Lambda q \qquad \forall i \tag{9}$$

where $\Lambda \in \Re^+$ denotes a constant scale factor used to match different scales between q and the UAV desired velocity u_i^u, and $q \in \Re^3$ denotes the position of end effector. In equation (9), multiple UAVs with an unbounded workspace can fly without the limitations of workspace by controlling the desired velocity using the configuration of the haptic device with a bounded workspace.

Simultaneously, to make the operator feel a telepresence of UAVs and their surrounding environments, we define the master–slave tracking error as defined by $q - (1/\Lambda N)\sum_{i=1}^{N} \dot{p}_i$ and the contact force acting on the slave side as defined by $(1/\Lambda N)\sum_{i=1}^{N} u_i^o$.

With these considerations, we define the force feedback control as follows

$$\tau = -B\dot{q} - Ky \tag{10}$$

where $B > 0$ and $K > 0$ are diagonal gain matrices, $-B\dot{q}$ represents a damping term, and $y \in \Re^3$ represents a haptic cue.

In addition, we consider the signal $y(t) \in \Re^3$ in terms of force-cue and velocity-cue feedback as defined by

$$y_f(t) := \frac{1}{\Lambda N}\sum_{i=1}^{N} u_i^o \tag{11}$$

$$y_v(t) := q - \frac{1}{\Lambda N}\sum_{i=1}^{N} \dot{p}_i \tag{12}$$

$$y(t) = y_f + y_v \tag{13}$$

where $\dot{p}_i$ denotes ith UAV's velocity, u_i^o denotes ith UAV's obstacle avoidance control input, $y_f(t)$ denotes force-cue feedback, and $y_v(t)$ denotes velocity-cue feedback. The force-cue feedback plays the role of a

repulsive force from the environment. It is related to the difference between the position of UAVs and the location of the obstacles. The velocity-cue feedback represents the difference between the commanded velocity as specified by q and the average velocity of UAVs. This difference is caused due to various reasons and is described in detail in the literature.[24,28–30] Finally, $y(t)$ denotes the sum of these two signals y_f and y_v and is sent to the master via the communication channel.

The ultimate objective involves implementing a multi-UAV system that enables a single operator to control N UAVs' Cartesian positions (1) $p := [p_1; p_2; \ldots; p_N] \in \Re^{3N}$ based on the distributed swarm control algorithm via the single 3-DOF haptic device (equation (8)) as shown in Figure 1. The operator teleoperates more intuitively by receiving visual feedback as well as haptic feedback based on the information of the N UAV's state and its surrounding environment (equation (13)).

Formation control, u_i^c. The second velocity term, $u_i^c \in \Re^3$denotes a control input to avoid a collision among UAVs, preserves connectivity, and achieves a certain desired formation as specified by the desired distances $d_{ij}^c \in \Re^+ \quad \forall i = 1, \ldots, N$, and $\forall j \in \mathcal{N}_i$, as defined by

$$u_i^c := -\sum_{j \in \mathcal{N}_i} \frac{\partial \varphi_{ij}^c(\parallel p_i - p_j \parallel^2)}{\partial p_i}^T \tag{14}$$

where φ_{ij}^c denotes a certain artificial potential function to create an attractive action if $\parallel p_i - p_j \parallel > d_{ij}^c$, a repulsive action if $\parallel p_i - p_j \parallel < d_{ij}^c$, and a null action if $\parallel p_i - p_j \parallel = d_{ij}^c$. The potential function φ_{ij}^c is described in further detail, and φ_{ij}^c consists of V_{ij} and W_{ij}.[31] V_{ij} denotes a repulsive potential function to avoid collision among UAVs and requires the following properties:

1. V_{ij} denotes a function of the square norm of the distance between UAVs i, j, not based on vector
$$V_{ij} = V_{ij}(\parallel p_i - p_j \parallel^2) = V_{ij}(\beta_{ij}) \tag{15}$$
2. V_{ij} attains its maximum value whenever $\beta_{ij} \to 0$. In other words, we require that $V_{ij} \to \infty$ whenever $\beta_{ij} \to 0$.
3. It is continuously differentiable from everywhere.
4. $\partial V_{ij}/\partial p_i = 0$ and $V_{ij} = 0$ whenever $\beta_{ij} > (d_{ij}^c)^2$.
5. $\partial V_{ij}/\partial \beta_{ij} < 0$ whenever $0 < \beta_{ij} < (d_{ij}^c)^2$, and $\partial V_{ij}/\partial \beta_{ij} = 0$ whenever $\beta_{ij} \geqslant (d_{ij}^c)^2$.

In addition, W_{ij} denotes an attractive potential function between UAVs i and $j \in \mathcal{N}_i$, which is required to exhibit the following properties for aggregation:

1. W_{ij} denotes a function of squared norm of the distance between UAVs i, j, that is not based on a vector
$$W_{ij} = W_{ij}(\parallel p_i - p_j \parallel^2) = W_{ij}(\beta_{ij}) \tag{16}$$
2. W_{ij} attains its maximum value whenever $\beta_{ij} \to \infty$. Thus, we require that $W_{ij} \to \infty$ whenever $\beta_{ij} \to \infty$.
3. It is continuously differentiable from everywhere.
4. $\partial W_{ij}/\partial p_i = 0$ and $W_{ij} = 0$ whenever $\beta_{ij} < (d_{ij}^c)^2$.
5. $\partial W_{ij}/\partial \beta_{ij} > 0$ whenever $(d_{ij}^c)^2 < \beta_{ij}$, and $\partial W_{ij}/\partial \beta_{ij} = 0$ whenever $\beta_{ij} \leqslant (d_{ij}^c)^2$.

Finally, the distributed formation control for each UAV i is given as the sum of the negative gradients of the two potentials, (equations (15) and (16)) in the p_i direction: $u_i^c := -\sum_{j \in \mathcal{N}_i} (\partial V_{ij}/\partial p_i) - \sum_{j \in \mathcal{N}_i} (\partial W_{ij}/\partial p_i)$. Therefore, given the presence of two vertical asymptotes in u_i^c about the bounded potential field, the prevention of intervehicle collisions and the preservation of intervehicle connectivity is guaranteed.

Obstacle avoidance control, u_i^o. The final velocity term, $u_i^o \in \Re^3$ c, is expressed by the following equation as a control input based on a potential field that allows multiple UAVs to avoid obstacles through a certain distance threshold $\mathcal{D}_o \in \Re^+$

$$u_i^o := -\sum_{r \in \mathcal{O}_i} \frac{\partial \varphi_{ir}^o(\parallel p_i - p_r^o \parallel)^T}{\partial p_i} \tag{17}$$

where $\mathcal{O}_i$ denotes the set of obstacles of the ith UAV with an obstacle point p_r^o that corresponds to the position of the rth obstacle in the environment, and φ_{ir}^o denotes a certain artificial potential function that produces a repulsive action if $\parallel p_i - p_r^o \parallel < \mathcal{D}_o$ and a null action if $\parallel p_i - p_r^o \parallel \geqslant \mathcal{D}_o$. When the distance between the UAVs and the obstacles becomes closer to D_o, then the repulsive potential function increases to infinity.

In short, each UAV is controlled by distributed swarm control (equation (6)), and this corresponds to the sum of the three control inputs. Although the first velocity term depends on the UAV control method, the operator inputs the desired velocity control commands to a multiple UAVs via a haptic device in the study (equation (9)). Second, with respect to the third velocity terms, a group of UAVs can automatically form the desired formation and avoid obstacles, (equations (14) and (17)). As a result, there are two control layers that consist of a teleoperation layer, which the operator inputs control commands via the haptic device, and a UAV control layer in which a slave's motion is controlled by the distributed swarm control algorithm. However, when autonomous UAVs are used, it exhibits a single control layer as shown in Figure 2.

Evaluation of distributed swarm control

Experimental setup

The apparatus mainly consists of a desktop, a monitor that displays the simulator, and a haptic device

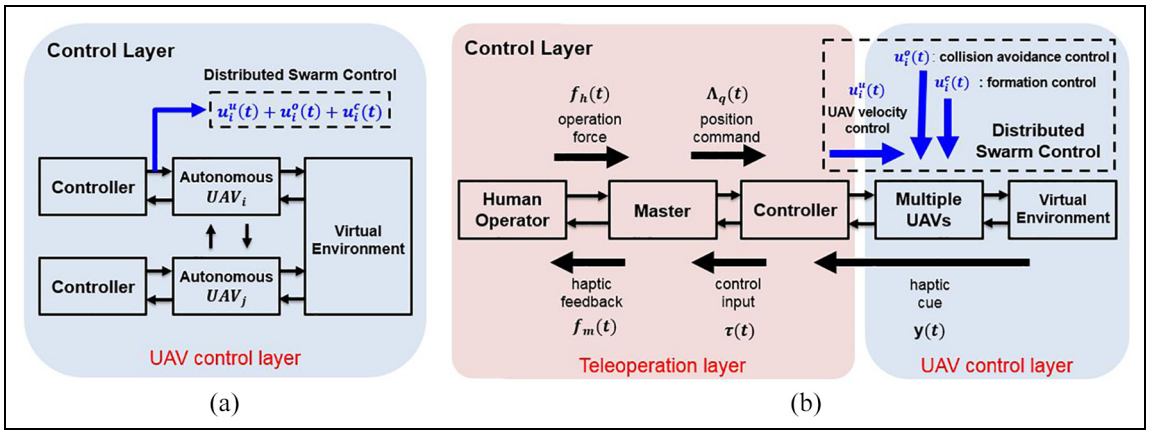

Figure 2. Control layer: (a) control layer when using an autonomous flight and (b) two control layers while using teleoperation.

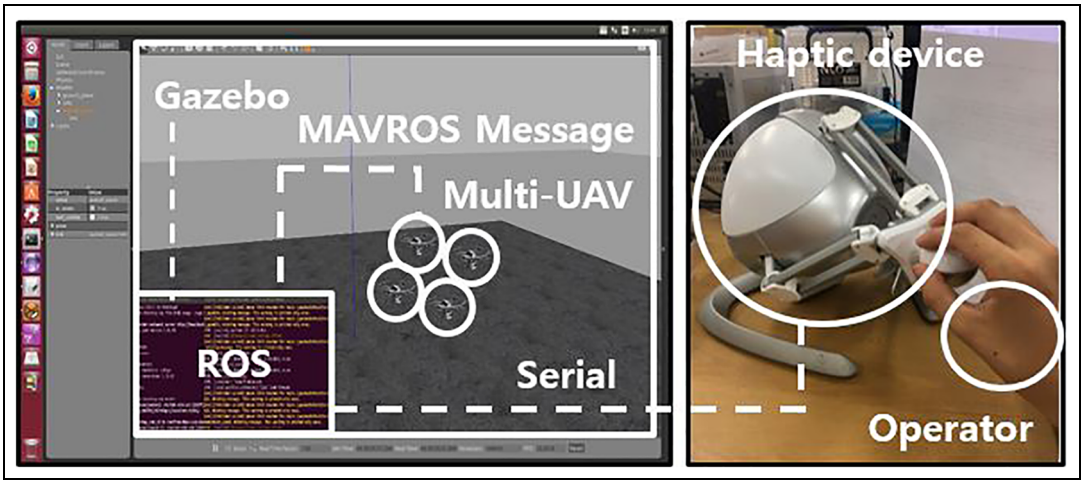

Figure 3. Experimental setup.

(Figure 3). In the desktop, we used the Ubuntu system to simulate the virtual environment using the robot operating system (ROS) and Gazebo (3D robot simulator). A virtual environment was constructed to simulate UAVs dynamics and their control laws. ROS is suitable for constructing and controlling robots and is suitable for constructing a swarm robot system because of its expandability and applicability.[32] The dynamical control of multiple UAVs based on the distributed swarm control algorithm was implemented in a virtual environment using Open Dynamics Engine (ODE). This environment was presented based on the Gazebo for 3D graphical rendering and on the ROS for haptic rendering, control, and communication. In the simulation, the visual scene is rendered from a camera perspective at a specific distance from the starting points of the UAVs. The graphic and haptic simulations are run at 60 and 1000 Hz, respectively.

In addition, an operator can control the virtual multi-UAV by manipulating the single haptic device. The haptic device is used as the master robot and corresponds to the Novint Falcon by Novint Technologies, Inc. with actuated linear 3-DOF and unactuated rotational 3-DOF. It generates 3-DOF force feedback up to 8.9 N at the nominal position, and its workspace is cube shaped with an edge ($4'' \times 4'' \times 4''$). The device is connected to a desktop through USB with 1000 Hz servo rate. Therefore, the desktop performs serial communication with the haptic device and communicates with the multiple UAVs through ROS messages (e.g. topics and services).

To run the *hardware-in-the-loop simulator*, we installed ROS, MAVROS package, Gazebo, and PX4/Firmware and used the Iris model for UAV that corresponds to an open source platform of 3DR. The Iris is created in the virtual Gazebo world via the ROS interface, and PX4 that corresponds to the firmware of Iris can simulate the virtual Iris by activating the micro air vehicle link (MAVLink) interface via the communication port. In the simulator, we used the MAVROS package by setting different MAVLink port values for each UAV, and MAVROS connected to the virtual Iris

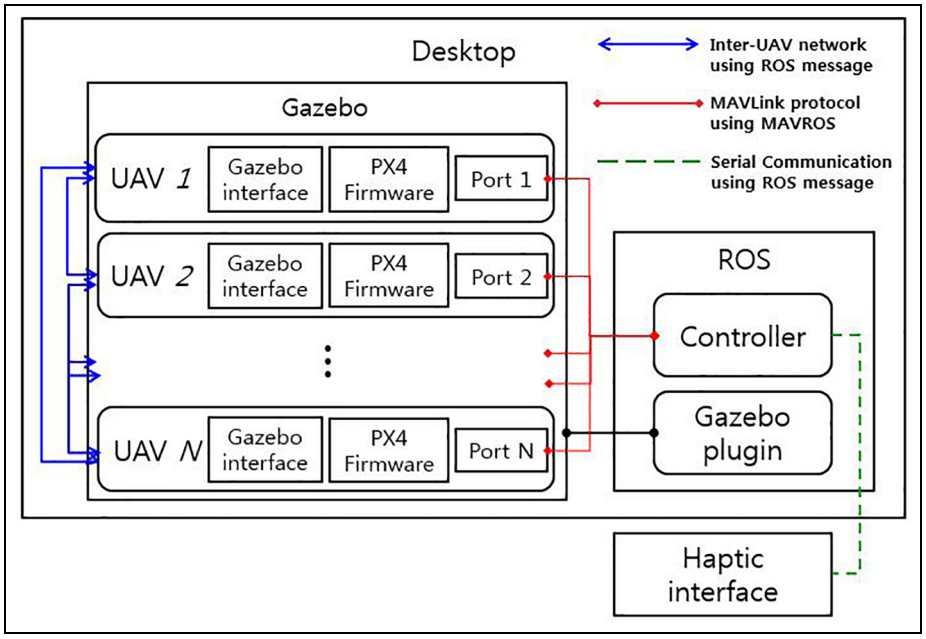

Figure 4. A block scheme of the hardware-in-the-loop simulation.

constructed the interface to control and communicate with Iris through ROS. As mentioned above, the communication method through MAVROS is the MAVLink protocol, and this is the same environment as that of the real UAV. The overall structure of the simulator is shown in Figure 4.

Experimental task

The experimental tasks involve the flight of a multiple UAVs based on the distributed swarm control algorithm along a specific path with respect to the operator's teleoperation command (Figure 5). In the experiments, we used four UAVs to implement swarm robot systems. During the experiments, we confirmed that multiple UAVs form the desired shape by the formation control. At this time, UAVs form a triangular pyramid with a constant relative distance (Figure 6). We also placed several obstacles in the path of the task and confirmed that the UAVs avoid collisions using the obstacle avoidance control. Here, the stereo camera is mounted on the UAV, and the obstacle is detected and the relative distance is measured by this stereo camera. As shown in the Figure 5, the path is defined until UAVs arrive at the goal area from the starting point, and the experiment ends when the multi-UAVs reach the goal area.

Data analysis

To confirm that the UAV forms well in the desired formation, avoids obstacles, and behaves in accordance with teleoperation commands, we recorded the position of the UAV(p_i), velocity of the UAV ($\dot{p}_i$), position of the obstacle (p_r^o), and simulation time (ms, t) at

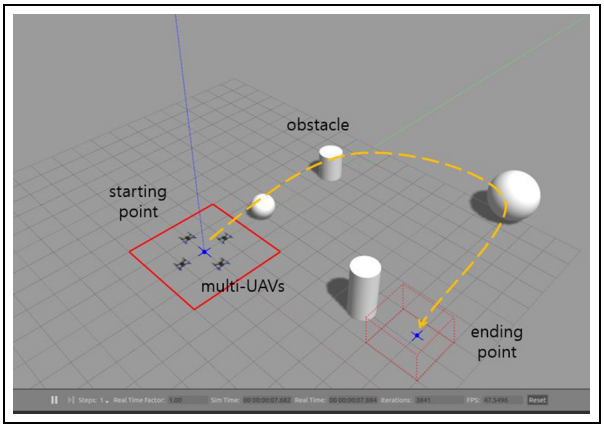

Figure 5. Experimental task.

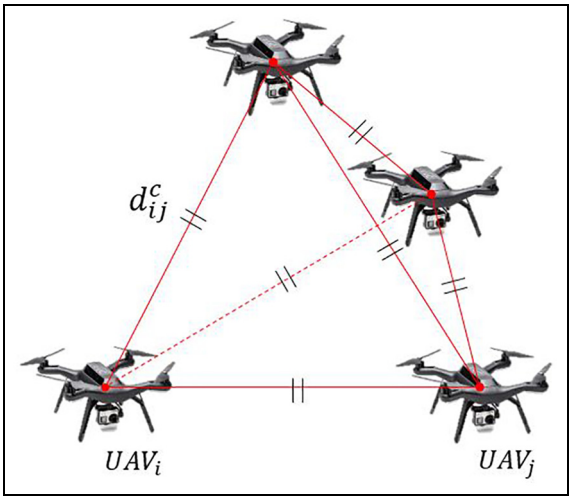

Figure 6. Formation of multiple UAVs.

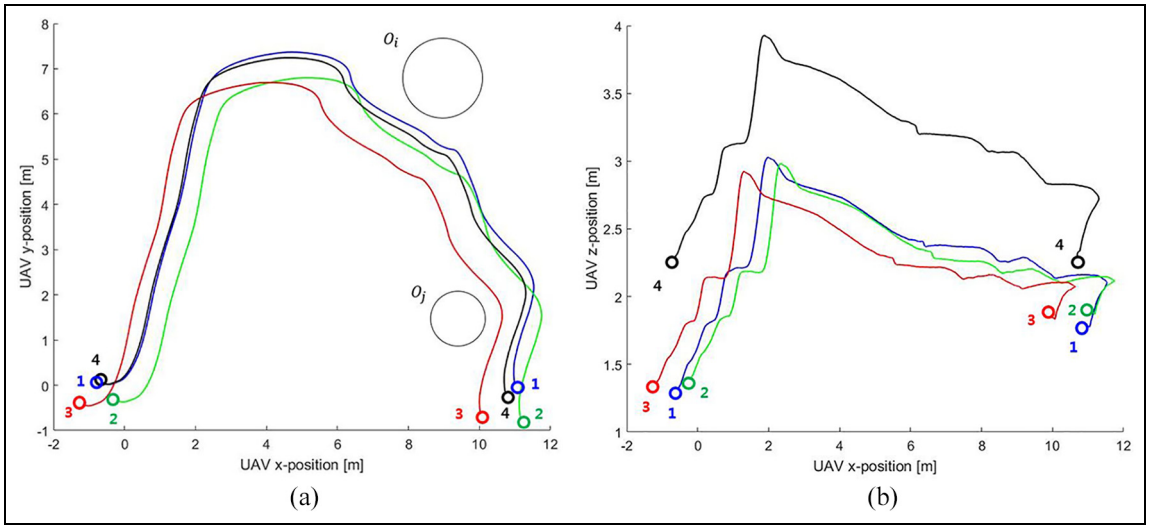

Figure 7. Trajectory of UAVs during the task: (a) XY plane and (b) XZ planes.

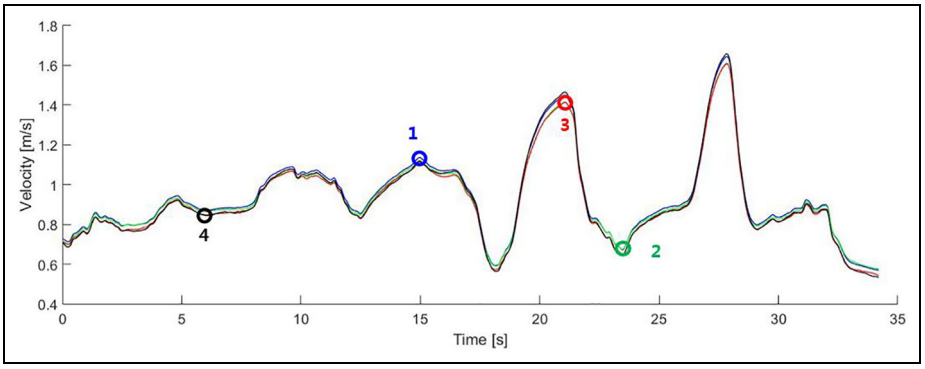

Figure 8. Velocity of UAVs $\dot{p}_i$.

1000 Hz. Most of the data were received via *rostopic*, and the *rosbag* was used to save the desired *rostopic*. Data analysis confirmed the following points: the multiple UAVs forms a shape of regular tetrahedron with a constant distance between each other, the UAVs are automatically avoided through repulsive action based on a potential field when the distance to the obstacle is less than the distance threshold, and it should act based on the operator's teleoperation commands. The results of the experiment are detailed in the following section.

Experimental results

In this study, the proposed distributed swarm control algorithm for an agricultural multi-UAV system is evaluated by performing an experiment that uses four UAVs. The distributed controllers are mounted on each UAV, and the teleoperation commands are transmitted to the multiple UAVs via Transmission Control Protocol/Internet Protocol (TCP/IP) communication. Although the controllers are implemented in a single computer during the experiment, the distributed swarm control algorithm is implemented in a distributed architecture.

In the experiments, a scenario was set wherein the operator controls the agricultural multi-UAV from the starting point to the ending point. Obstacles, such as trees and utility poles, are placed in the field, and the agricultural task proceeds such that it passes above or beside the obstacles. Here, the multiple UAVs are assumed as a UAV for agricultural tasks involving crop observation, spraying, or sowing. The experimental results are shown in Figures 7–10.

In Figure 7, we present the positions of multiple UAVs during the experiment. This figure shows the trajectories of the UAVs controlled by the operator's teleoperation command and indicate as to whether the UAVs form the desired formation. The multiple UAVs are controlled by the distributed swarm control algorithm, and the formation is well shaped as shown in Figures 6 and 7. Therefore, when the multiple UAVs are applied to the agricultural tasks using this algorithm, the operator can perform work while maintaining the desired formation of UAVs. In addition, the operator controls via teleoperation, and thus, it is possible to work more precisely on the desired area and also to cope with an unexpected accident. Furthermore, the

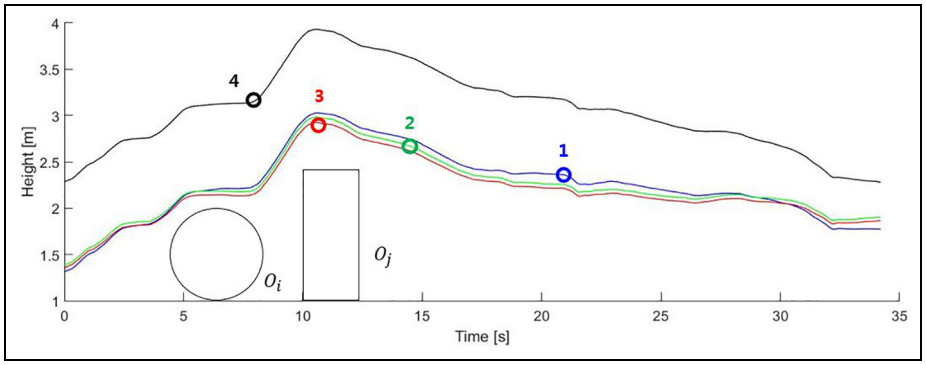

Figure 9. Height of UAVs with obstacles.

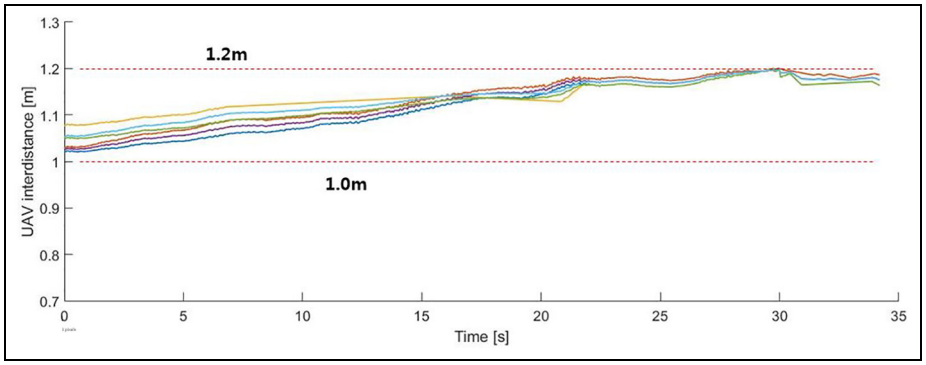

Figure 10. Relative distance between UAVs $\| p_i - p_j \|$.

formation of multi-UAV is controlled by modifying the artificial potential function to form the desired formation, and it is possible to perform a flexible task by forming a one-column-array shape or a quadrilateral shape as necessary. These results indicate that the agricultural multiple UAVs can avoid obstacles and fly to the desired area while forming a desired formation.

Figure 8 shows the velocity of each UAV. In this case, the velocity control is input to each UAV as the sum of the teleoperation control, formation control, and collision avoidance control. In this experiment, the largest input corresponds to the velocity control by a teleoperation command, and the supplementary inputs correspond to the formation control and the collision avoidance control. The distributed swarm control is represented by the sum of three control inputs, and thus, the formation may change based on the control input that is mainly applied. It may not be controlled as desired, and thus, it is necessary to consider the most important control input. As shown in the figure, the three control inputs control each UAV, and agricultural work is performed uniformly and constantly because the velocity of each UAV does not significantly differ. This result also means that the formation of the multi-UAV system flies at a uniform speed without collapsing, so that specific areas are not oversaturated for agricultural tasks.

Figure 9 represents the height of the UAVs and the position of the obstacles. This result means that multiple UAVs were affected by the collision avoidance control. In the simulation, the multi-UAV approaches upward with respect to the first and second obstacles and approaches the side of the middle for the other two obstacles. This result is influenced by the teleoperation command to move forward and the obstacle avoidance control to push to the opposite side. However, the teleoperation command is larger than obstacle avoidance control, so the multiple UAVs are moved forward and upward. As shown in the figure, when the distance between the UAVs and the obstacles is within a certain distance threshold, the repulsive potential field increases while approaching the obstacle, and multiple UAVs avoid the obstacles. In this method, it is possible to avoid the increasingly frequent crashing problem caused by the collision with the utility pole when the algorithm is applied to an agricultural multi-UAV system and to safely avoid specific obstacles when the obstacles are detected by a sensor during agricultural tasks.

Figure 10 indicates the relative distances between UAVs, and this result is mainly affected by the formation control. Theoretically, it is necessary to maintain a relative distance between UAVs at a certain desired distance although it is almost impossible to be the same. This is because the position measurement errors occur at times, the UAVs may become unstable due to disturbance and communication delay, and the position of the UAVs constantly changes. Thus, it is impossible to match the accurate value. Therefore, in the simulator, the relative distance between UAVs is maintained at a

distance between 1 and 1.2 m. Hence, specification of the desired range between UAVs in this manner prevents oscillation by the potential field more than that when the relative distance between UAVs is set to be a desired distance. The repulsive action was derived when the distance between the UAVs became closer to 1 m, and the attractive action was derived when the distance between the UAVs exceeds 1.2 m such that the formation is maintained. As shown in the figure, the distance between the UAVs does not exceed 1.2 m and is not below 1 m. These results represent that the proposed multi-UAV system is stable and safety. Therefore, even if multiple UAVs are used in an agricultural system when compared with a conventional system that uses a single UAV, it can be controlled stably because it maintains the desired formation while avoiding collision with others. The multiple UAVs work together, and this simultaneously increases the amount of workload and the work area, reduces the completion time, and significantly increases the agricultural efficiency.

Conclusion

In this study, we proposed a distributed swarm control algorithm for agricultural multiple UAVs using a teleoperation architecture that consisted of the following two layers: (1) a UAV control layer that controls the multiple UAVs to form a desired formation as specified by the desired distances to avoid obstacles specified by the distance threshold and to drive a specific path by UAV control method and (2) a teleoperation layer that controls multiple UAVs such that they move at a desired velocity given the operator's teleoperation command, and the operator simultaneously receives haptic feedback with respect to sensing UAVs and their surrounding obstacles. To apply the same to actual agricultural multi-UAV systems, we used a teleoperation method for UAV control and a distributed method for swarm control, and the methods are optimized for the agricultural environment. In a distributed swarm control algorithm, the sum of control inputs including a UAV control input using teleoperation, a formation control input to form a desired formation using an artificial potential field, and a collision avoidance control input to automatically avoid obstacles using a potential field was applied to each UAV for the distributed system. In addition, we implemented a multi-UAV system into a hardware-in-the-loop simulator using ROS and a Gazebo to evaluate and validate the proposed algorithm. The experimental results proved that the distributed swarm control algorithm can be applied to a multi-UAV system for agricultural tasks, and it improves work efficiency when compared with that of a conventional single UAV system. In addition, it is possible to safely perform the agricultural tasks because multiple UAVs avoid obstacles while maintaining the desired distance between UAVs. It is also applied to agricultural multiple ground robots as well as UAVs.

Several possible future research directions include the following: (1) implementation of a multi-UAV system based on a distributed swarm control algorithm using a real UAV, (2) application of various experimental scenarios for agricultural work, and (3) comparison and analysis of simulation results and experimental results using a real multi-UAV system. If an agricultural multi-UAV system based on distributed swarm control is implemented using real UAVs, then it can be applied to general agricultural tasks including pest detection, spraying and sowing, and crop monitoring by utilizing various onboard devices and sensors. Furthermore, it significantly contributes to reducing labor and in potentially alleviating food shortage problems in the future.

Declaration of conflicting interests

The author(s) declared no potential conflicts of interest with respect to the research, authorship, and/or publication of this article.

Funding

The author(s) disclosed receipt of the following financial support for the research, authorship, and/or publication of this article: This research was supported, in part, by the Basic Science Research Program through the National Research Foundation of Korea (NRF) funded by the Ministry of Science, ICT & Future Planning (grant no. NRF-2018R1D1A1B07046948); in part, by Korea Institute of Planning and Evaluation for Technology in Food, Agriculture, Forestry (IPET) through Advanced Production Technology Development Program, funded by Ministry of Agriculture, Food and Rural Affairs (MAFRA; 115062-2); and, in part, by the Technology Innovation Program (10076868) funded by the Ministry of Trade, Industry & Energy.

ORCID iD

Hyoung Il Son https://orcid.org/0000-0002-7249-907X

References

1. King A. Technology: the future of agriculture. *Nature* 2017; 544(7651): S21–S23.
2. Freeman PK and Freeland RS. Agricultural UAVs in the U.S.: potential, policy, and hype. *Remote Sens Appl Soc Env* 2015; 2: 35–43.
3. Das J, Cross G, Qu C, et al. Devices, systems, and methods for automated monitoring enabling precision agriculture. In: *Proceedings of the 2015 IEEE international conference on automation science and engineering (CASE)*, Gothenburg, 24–28 August 2015, pp.462–469. New York: IEEE.
4. Candiago S, Remondino F, De Giglio M, et al. Evaluating multispectral images and vegetation indices for

precision farming applications from UAV images. *Remote Sens* 2015; 7(4): 4026–4047.
5. Katsigiannis P, Misopolinos L, Liakopoulos V, et al. An autonomous multi-sensor UAV system for reduced-input precision agriculture applications. In: *Proceedings of the 2016 24th Mediterranean conference on control and automation (MED)*, Athens, 21–24 June 2016, pp.60–64. New York: IEEE.
6. Xiang H and Tian L. Development of a low-cost agricultural remote sensing system based on an autonomous unmanned aerial vehicle (UAV). *Biosyst Eng* 2011; 108(2): 174–190.
7. Doering D, Benenmann A, Lerm R, et al. Design and optimization of a heterogeneous platform for multiple UAV use in precision agriculture applications. *IFAC P Vol* 2014; 47(3): 12272–12277.
8. Beckers R, Holland O and Deneubourg JL. From local actions to global tasks: stigmergy and collective robotics. In: Brooks RA and Maes P (eds) *Artificial life IV: proceedings of the fourth international workshop on the synthesis and simulation of living systems*. Cambridge, MA: The MIT Press, 1994, pp.181–189.
9. Jones C, Shell D, Mataric MJ, et al. Principled approaches to the design of multi-robot systems. In: *Proceedings of the workshop on networked robotics IEEE/RSJ international conference on intelligent robots and systems (IROS-04)*, Sendai, Japan, 24 September–2 October 2004, pp.71–80. IEEE.
10. Ju C and Son HI. Performance evaluation of multiple UAV systems for remote sensing in agriculture. In: *Proceedings of the workshop on robotic vision and action in agriculture at the 2018 IEEE international conference on robotics and automation (ICRA)*, Brisbane, QLD, Australia, 21–26 May 2018, pp.21–26. New York: IEEE.
11. Ju C and Son HI. Multiple UAV systems for agricultural applications: control, implementation, and evaluation. *Electronics* 2018; 7(9): 162.
12. Merino L, Caballero F, Martnez-de Dios JR, et al. A cooperative perception system for multiple UAVs: application to automatic detection of forest fires. *J Field Robot* 2006; 23(3–4): 165–184.
13. Han J, Xu Y, Di L, et al. Low-cost multi-UAV technologies for contour mapping of nuclear radiation field. *J Intell Robot Syst* 2013; 70(1–4): 401–410.
14. Ahmadzadeh A, Jadbabaie A, Kumar V, et al. Multi-UAV cooperative surveillance with spatio-temporal specifications. In: *Proceedings of the 2006 45th IEEE conference on decision and control*, San Diego, CA, 13–15 December 2006, pp.5293–5298. New York: IEEE.
15. Chao H, Baumann M, Jensen A, et al. Band-reconfigurable multi-UAV-based cooperative remote sensing for real-time water management and distributed irrigation control. *IFAC P Vol* 2008; 41(2): 11744–11749.
16. Lee D, Franchi A, Giordano PR, et al. Haptic teleoperation of multiple unmanned aerial vehicles over the internet. In: *Proceedings of the 2011 IEEE international conference on robotics and automation (ICRA)*, Shanghai, China, 9–13 May 2011, pp.1341–1347. New York: IEEE.
17. Franchi A, Giordano PR, Secchi C, et al. A passivity-based decentralized approach for the bilateral teleoperation of a group of UAVs with switching topology. In: *Proceedings of the 2011 IEEE international conference on robotics and automation (ICRA)*, Shanghai, China, 9–13 May 2011, pp.898–905. New York: IEEE.
18. Franchi A, Secchi C, Son HI, et al. Bilateral teleoperation of groups of mobile robots with time-varying topology. *IEEE T Robot* 2012; 28(5): 1019–1033.
19. Lee D, Franchi A, Son HI, et al. Semiautonomous haptic teleoperation control architecture of multiple unmanned aerial vehicles. *IEEE-ASME T Mech* 2013; 18(4): 1334–1345.
20. Franchi A, Secchi C, Ryll M, et al. Shared control: balancing autonomy and human assistance with a group of quadrotor UAVs. *IEEE Robot Autom Mag* 2012; 19(3): 57–68.
21. Avellar GS, Pereira GA, Pimenta LC, et al. Multi-UAV routing for area coverage and remote sensing with minimum time. *Sensors* 2015; 15(11): 27783–27803.
22. Borrelli F, Keviczky T and Balas GJ. Collision-free UAV formation flight using decentralized optimization and invariant sets. In: *Proceedings of the 2004 43rd IEEE conference on decision and control (CDC) (volume 1)*, Nassau, Bahamas, 14–17 December 2004, pp.1099–1104. New York: IEEE.
23. Yang H, Lee Y, Jeon SY, et al. Multi-rotor drone tutorial: systems, mechanics, control and state estimation. *Intel Serv Robot* 2017; 10(2): 79–93.
24. Son HI, Franchi A, Chuang LL, et al. Human-centered design and evaluation of haptic cueing for teleoperation of multiple mobile robots. *IEEE Trans Cybern* 2013; 43(2): 597–609.
25. Grzonka S, Grisetti G and Burgard W. A fully autonomous indoor quadrotor. *IEEE T Robot* 2012; 28(1): 90–100.
26. Sujit P, Saripalli S and Sousa JB. Unmanned aerial vehicle path following: a survey and analysis of algorithms for fixed-wing unmanned aerial vehicles. *IEEE Contr Syst Mag* 2014; 34(1): 42–59.
27. Rodriguez-Seda EJ, Troy JJ, Erignac CA, et al. Bilateral teleoperation of multiple mobile agents: coordinated motion and collision avoidance. *IEEE T Contr Syst T* 2010; 18(4): 984–992.
28. Son HI, Kim J, Chuang L, et al. An evaluation of haptic cues on the tele-operator's perceptual awareness of multiple UAVs' environments. In: *Proceedings of the 2011 IEEE world haptics conference (WHC)*, Istanbul, 21–24 June 2011, pp.149–154. New York: IEEE.
29. Son HI, Chuang LL, Franchi A, et al. Measuring an operator's maneuverability performance in the haptic teleoperation of multiple robots. In: *Proceedings of the 2011 IEEE/RSJ international conference on intelligent robots and systems (IROS)*, San Francisco, CA, 25–30 September 2011, pp.3039–3046. New York: IEEE.
30. Ju C and Son HI. Evaluation of haptic feedback in the performance of a teleoperated unmanned ground vehicle in an obstacle avoidance scenario. *Int J Control Autom* 2019; 17(1): 168–180.
31. Dimarogonas DV and Kyriakopoulos KJ. Connectedness preserving distributed swarm aggregation for multiple kinematic robots. *IEEE T Robot* 2008; 24(5): 1213–1223.
32. Ladosz P, Coombes M, Smith J, et al. A generic ROS based system for rapid development and testing of algorithms for autonomous ground and aerial vehicles. In: Koubaa A (ed.) *Robot operating system (ROS)*. Cham: Springer, 2019, pp.113–153.